Journal of Inorganic and General Chemistry
ZAAC
Zeitschrift für anorganische und allgemeine Chemie
DOI: 10.1002/zaac.201900360
ARTICLE

The Triclinic Lanthanoid(III) Halide Oxidoarsenates(III) $Sm_3Cl_2[As_2O_5][AsO_3]$ and $Tm_3Br_2[As_2O_5][AsO_3]$

Felix C. Goerigk,[a] Svetlana Schander,[b] Mathias S. Wickleder,[c] and Thomas Schleid*[a]

Dedicated to Professor Manfred Scheer to the Occasion of his 65th Birthday

Abstract. Pale yellow single crystals of the composition $Ln_3X_2[As_2O_5][AsO_3]$ (Ln = Tm for X = Br and Ln = Sm for X = Cl) were obtained via solid-state reactions in the systems Ln_2O_3/As_2O_3 from sealed silica ampoules using different halides as fluxing agents. $Sm_3Cl_2[As_2O_5][AsO_3]$ and $Tm_3Br_2[As_2O_5][AsO_3]$ crystallize isotypically in the triclinic space group $P\bar{1}$ with Z = 2 and cell parameters of a = 543.51(4) pm, b = 837.24(6) pm, c = 1113.45(8) pm, α = 90.084(2)°, β = 94.532(2)°, γ = 90.487(2)° for the samarium and a = 534.96(4) pm, b = 869.26(6) pm, c = 1081.84(8) pm, α = 90.723(2)°, β = 94.792(2)° γ = 90.119(2)° for the thulium compound. The isotypic crystal structure of both representatives exhibits three crystallographically different Ln^{3+} cations, each with a coordination number of eight. $(Ln1)^{3+}$ and $(Ln2)^{3+}$ are only coordinated by three oxygen atoms, whereas $(Ln3)^{3+}$ shows additional contacts to halide anions in forming square $[LnO_4X_4]^{9-}$ antiprisms. All As^{3+} cations are surrounded by three oxygen atoms in the shape of isolated $[AsO_3]^{3-}$ ψ^1-tetrahedra. They occur either isolated or condensed as pyroanionic $[As_2O_5]^{4-}$ units with a bridging oxygen atom. In both anions, non-binding lone-pair electrons are present at the As^{3+} cations with a pronounced stereochemically active function.

Introduction

Rare-earth metal(III) oxidophosphates(V) with the composition $RE[PO_4]$ represent one of the main sources for the rare-earth metals and have been subject of interest regarding the occurring crystal structures. Two modifications, namely the monoclinic *monazite* type for the lighter rare-earth elements (RE = La – Tb) and the tetragonal *xenotime* type for the heavier ones (RE = Tb – Lu and Y) are known.[1–3] High-pressure conditions transform them into the *scheelite*-type crystal structure.[4] Moreover, with appropriate lanthanoid dopants (Ln = Eu and Tb) in suitable hosts (La[PO_4] and Y[PO_4]), these phosphates even turn into phosphors for lighting applications.[5]

For arsenic being the heavier homologue of phosphorus, further investigations of possible similarities in the crystal structures of the $Ln[AsO_4]$ compounds compared to the $Ln[PO_4]$ congeners were of interest. Y[AsO_4], the first ternary rare-earth metal(III) oxidoarsenate(V), was described crystallizing with the *xenotime*-type structure in the year 1934.[6] The elucidation of the structures of the remaining rare-earth metal(III) oxidoarsenates(V) followed in subsequent decades. They were found crystallizing either in the *monazite*-type (Ln = La – Nd) or the *xenotime*-type (Ln = Y, Sm – Lu) and even the *scheelite*-type structure became evident as high-pressure modification.[1,7] Rare-earth metal containing compounds with complex oxidoanions, such as oxidoarsenates, are always a promising material class for possible luminescence properties due to their ligand-to-metal charge-transfer effects.[8]

While oxidophosphates(III) of the rare-earth metals are not known up to now, the first ternary, halide-free rare-earth metal(III) oxidoarsenates(III) were reported for the first time in 2005 with the empirical formula $Ln_2As_4O_9$ ($\equiv {}^1/_2\ Ln_4[As_2O_5]_2[As_4O_8]$ with Ln = Pr, Nd and Sm) exhibiting both $[As_2O_5]^{4-}$ pyroanions and cyclic $[As_4O_8]^{4-}$ units as condensation products of two and four $[AsO_3]^{3-}$ ψ^1-tetrahedra, respectively.[9,10] The influence of the non-binding electron pairs at the As^{3+} cations on the crystal structure was also further investigated in 2012, when the first simple ternary compounds $Ln[AsO_3]$ with Ln = La and Ce showing isolated $[AsO_3]^{3-}$ units followed.[11,12] For the examples $Ln[AsO_3]$, only discrete $[AsO_3]^{3-}$ anions are present. Up to now, no further crystal structures of the heavier ternary rare-earth metal(III) oxidoarsenates(III) with the composition $Ln[AsO_3]$ are known.

The addition of different fluxing agents such as binary halides in order to improve the crystal growth delivered different quaternary halide-containing compounds, since these fluxes both provided a salt melt at high temperatures and parts of the melt were incorporated in the synthesized compounds. The first members for the lighter lanthanoids of the series $Ln_5Cl_3[AsO_3]_4$ with Ln = La – Nd and Sm have been reported

* Prof. Dr. Th. Schleid
E-Mail: schleid@iac.uni-stuttgart.de
[a] Institute for Inorganic Chemistry
University of Stuttgart
70569 Stuttgart, Germany
[b] Institute for Pure and Applied Chemistry
University of Oldenburg
26129 Oldenburg, Germany
[c] Institute for Inorganic Chemistry
University of Cologne
50939 Cologne, Germany

in 2006 and recently discussed again with regard to their syntheses and crystal structures. Moreover, the fluoride-containing quaternary compounds $Ln_5F_3[AsO_3]_4$ with *RE* = Y, Yb and Lu are known as representatives for the heavier rare-earth metals crystallizing with a non-isotypic tetragonal structure in contrast to the monoclinic chloride congeners.[13–16] With additional oxide anions, the series $Ln_3OX[AsO_3]_2$ with *Ln* = La – Pr and Eu – Dy for *X* = Cl and *Ln* = La, Ce, Nd, Sm, Gd and Tb for *X* = Br as well as $Ln_5O_4Cl[AsO_3]_2$ with *Ln* = Nd and Pr can be observed.[16–22] In both crystal structures, only isolated $[AsO_3]^{3-}$ anions with stereochemically active, non-binding electron pairs are present.

With the following work, the structural diversity of rare-earth metal(III) oxidoarsenates(III) could be extended to the new composition $Ln_3X_2[As_2O_5][AsO_3]$ for both chloride- and bromide- containing examples. With $Tm_3Br_2[As_2O_5][AsO_3]$ it was furthermore possible to describe the first quaternary halide-containing thulium(III) oxidoarsenate(III) as representative for one of the heaviest lanthanoids. The present work deals with the synthesis and crystal structure of both $Sm_3Cl_2[As_2O_5][AsO_3]$ and $Tm_3Br_2[As_2O_5][AsO_3]$ as hitherto unprecedented lanthanoid(III) oxidoarsenates(III) containing both the structural features of isolated and condensed oxidoarsenate(III) units as $[AsO_3]^{3-}$ and $[As_2O_5]^{4-}$ anions so far.

Results and Discussion

The compounds with the composition $Ln_3X_2[As_2O_5][AsO_3]$ (*Ln* = Sm for *X* = Cl and *Ln* = Tm for *X* = Br) crystallize isotypically in the triclinic centrosymmetric space group $P\bar{1}$ with cell parameters like *a* = 543.51(4) pm, *b* = 837.24(6) pm, *c* = 1113.45(8) pm, *α* = 90.084(2)°, *β* = 94.532(2)°, *γ* = 90.487(2)° for the samarium and *a* = 534.96(4) pm, *b* = 869.27(6) pm, *c* = 1080.79(8) pm, *α* = 90.701(2)°, *β* = 94.789(2)° and *γ* = 90.158(2)° for the thulium compound. With *Z* = 2, the crystal structure exhibits three crystallographically different 2*i*-positions for the Ln^{3+} cations. Both $(Ln1)^{3+}$ and $(Ln2)^{3+}$ are eightfold coordinated exclusively by oxygen atoms building up distorted square $[(Ln1,2)O_8]^{13-}$ prisms or antiprisms, respectively (Figure 1). The lanthanoid-oxygen bonds (*Ln*1,2)–O feature lengths of 221–253 pm for $(Ln1)^{3+}$ and 223–261 pm for $(Ln2)^{3+}$ and fall therefore in a similar range as the corresponding distances for samarium sesquioxide (Sm_2O_3, b*ixbyite* type), samarium oxide chloride (SmOCl, *matlockite* type), thulium sesquioxide (Tm_2O_3, b*ixbyite* type) and thulium oxide bromide (TmOBr, *matlockite* type), where values of 230–242 pm[23,24] for *Ln* = Sm and 222–256 pm[25,26] for *Ln* = Tm are found.

In contrast, $(Ln3)^{3+}$ is the only lanthanoid(III) cation with contacts to halide anions (Figure 2). Four oxygen atoms and four halide anions establish a square antiprism around $(Ln3)^{3+}$, where bond lengths of *d*(*Ln*3–O) = 220–259 pm and *d*(*Ln*3–*X*) = 274–322 pm occur. These distances are also in accordance with literature-known values for samarium-chloride as well as thulium-bromide bonds, e.g. *d*(Sm–Cl) = 286–291 pm in $SmCl_3$ (UCl_3 type)[27] and 309–312 pm in SmOCl,[23] *d*(Tm–Br) = 295 pm in TmOBr[26] and 283–290 pm in $TmBr_3$

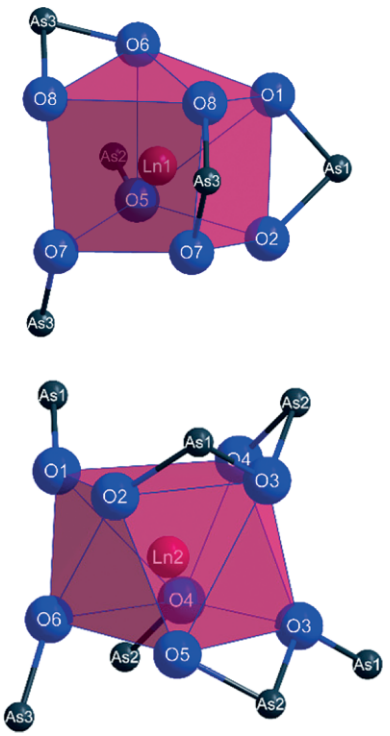

Figure 1. Coordination polyhedra of the $(Ln1)^{3+}$ (top) and $(Ln2)^{3+}$ (bottom) cations built up by eight oxygen atoms in the shape of distorted $[LnO_8]^{13-}$ square prisms or antiprisms with the As^{3+} cations in contact to their covalently bonded oxygen atoms.

($FeCl_3$ type).[28] Table 3 offers a compilation of all relevant bond lengths.

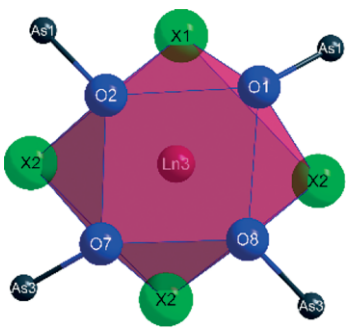

Figure 2. Coordination polyhedron of the $(Ln3)^{3+}$ cation built up by four oxygen atoms and four halide anions in the shape of a square $[(Ln3)O_4X_4]^{9-}$ antiprism with the As^{3+} cations in contact to their covalently bonded oxygen atoms.

The occurring $[(Ln1,2)O_8]^{13-}$ polyhedra build up infinite layers in the *ac* plane via oxygen edge-connection (Figure 3). The $(Ln3)^{3+}$ cations, grafted by their involved oxygen atoms to these layers, reside above and below these sheets. Their $[(Ln3)O_4X_4]^{9-}$ antiprisms themselves are edge-connected via common halide anions with *cis*-edge orientation building up strands along the *a* axis (Figure 4). The interconnection of these strands is caused by mutual edges of shared oxygen atoms forming double strands according to $^1_\infty\{[LnO_{4/1}(X1)_{1/1}(X2)_{3/3}]^{7-}\}$ in positions between the layers of the fused $[(Ln1,2)O_8]^{13-}$ polyhedra.

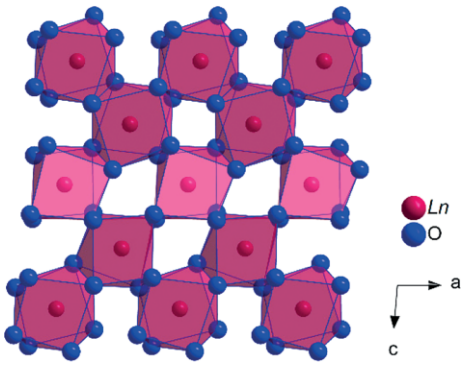

Figure 3. Infinite layer of edge-connected $[(Ln1,2)O_8]^{13-}$ polyhedra spreading out parallel to the (010) plane.

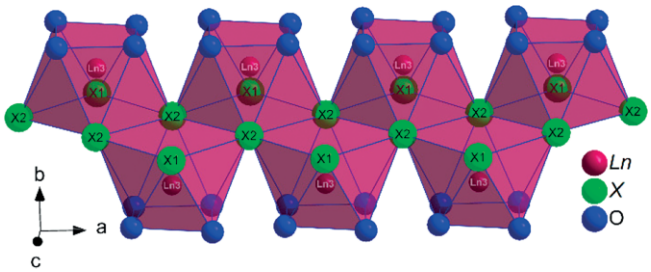

Figure 4. One-dimensional infinite double strand of edge-connected square $[(Ln3)O_4X_4]^{9-}$ antiprisms propagating along the *a* axis.

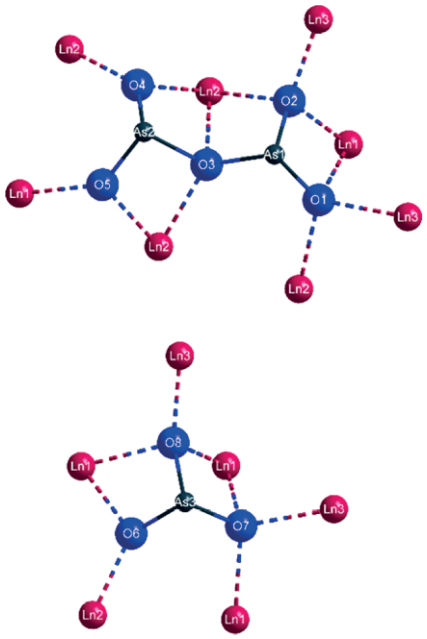

Figure 5. Coordination spheres of the $(As1)^{3+}$, $(As2)^{3+}$ and $(As3)^{3+}$ cations built up by three oxygen atoms in the shape of $[AsO_3]^{3-}$ ψ^1-tetrahedra, which are vertex-connected to pyroanionic $[As_2O_5]^{4-}$ units (top) and isolated $[AsO_3]^{3-}$ anions for (As3) (bottom). Their periphery of Ln^{3+} cations is also shown in both cases.

The halide anions show different coordination spheres, since $(X1)^-$ has only one binding connection to a $(Ln3)^{3+}$ cation with a bond length of 274 or 285 pm, while $(X2)^-$ is coordinated threefold by $(Ln3)^{3+}$ cations in a triangular shape, where the central $(X2)^-$ anion is deflected with 88 pm (for the samarium compound) or 92 pm (for the thulium compound) from the plane of the three lanthanoid(III) cations.

The structure contains three crystallographically different positions for the As^{3+} cations. $(As1)^{3+}$ and $(As2)^{3+}$ are surrounded by five oxygen atoms building up a pyroanionic $[As_2O_5]^{4-}$ unit (Figure 5, top). The oxygen atoms O1 and O2 show contacts to three Ln^{3+} cations, while O4 and O5 only have two contacts to Ln^{3+} cations. Therefore, the arsenic-oxygen distances to the former oxygen atoms are slightly longer with values of d(As1–O1) ≈ 177 pm and d(As1–O2) ≈ 184 pm as compared with the ones with fewer contacts to Ln^{3+} cations showing separations of d(As2–O4) ≈ 175 pm and d(As2–O5) ≈ 176 pm. O3 is the only oxygen atom with contact to both As^{3+} cations with bond lengths of d(As1–O3) ≈ 186 pm or d(As2–O3) ≈ 196 pm and therefore shows the largest values. In comparison to halide-free oxidoarsenates(III) such as $Sm_2As_4O_9$, where arsenic-oxygen bond lengths of 186–188 pm for the bridging oxygen atoms in the $[As_2O_5]^{4-}$ unit are present, the occurring distances in the $Ln_3X_2[As_2O_5][AsO_3]$ compounds are remarkably unequal.[10] Further comparisons of this aspect with the transition-metal oxidoarsenate(III) $Mn_2[As_2O_5]$ which also features pyroanionic $[As_2O_5]^{4-}$ units, show arsenic-oxygen distances of 183–184 pm and 186–187 pm for the bridging oxygen atoms.[29] These nearly equally distributed bond lengths are in good accordance to the ones in $Sm_2As_4O_9$ and emphasize the uncommon nature of the asymmetric $[O_2(As1)–(O3)–(As2)O_2]^{4-}$ unit in the here presented crystal structure.

The third arsenic cation, $(As3)^{3+}$, is surrounded by three oxygen atoms establishing an isolated ψ^1-tetrahedral $[AsO_3]^{3-}$ anion, where O6 has only contact to two Ln^{3+} cations and hence a shorter distance to $(As3)^{3+}$ with d(As3–O6) ≈ 175 pm as compared with the oxygen atoms (O7 and O8) with contacts to three Ln^{3+} cations and bond lengths of d(As3–O7) ≈ 180 pm and d(As3–O8) ≈ 184 pm (Figure 5, bottom).

These distances fall in a similar range as the arsenic-oxygen bond lengths in *claudetite-I*, *claudetite-II* and *arsenolite*, the common crystalline modifications of As_2O_3, displaying values of 172–181 pm,[30] 177–182 pm[31] and 179 pm, respectively.[32]

In comparison to hitherto described crystal structures of lanthanoid(III) halide oxidoarsenates(III), outstanding similarities can be observed. The monoclinic oxidoarsenates(III) with the composition $Ln_5Cl_3[AsO_3]_4$ (*Ln* = La – Nd and Sm) exhibit an alternating stacking of the present oxide and halide layers in the crystal structure with different crystallographic positions for the Ln^{3+} cations.[13] In the crystal structures of the $Ln_5Cl_3[AsO_3]_4$ representatives, *Ln*1 and *Ln*2 are only coordinated by oxygen atoms with a coordination number of eight, whereas *Ln*3 exhibits a (4+4)-fold coordination of four oxygen atoms and four chloride anions. This leads to the formation of alternating anion layers along the *a*-axis. In the structure of the $Ln_3X_2[As_2O_5][AsO_3]$ compounds, a comparable behavior can be observed, since also three different crystallographic positions for the lanthanoid(III) cations are present. *Ln*1 and *Ln*2 show an exclusive coordination by oxygen atoms, whereas *Ln*3

has a coordination sphere of four oxygen atoms and four halide anions, very similar to the coordination of *Ln*3 in the monoclinic $Ln_5Cl_3[AsO_3]_4$ compounds. This fact leads to an alternative layering of the oxygen atoms and halide anions (Figure 6) along the *b* axis. In direct comparison of the linking patterns of the coordination polyhedra around $(Ln3)^{3+}$, the formation of one-dimensional strands $^1_\infty\{[Ln3)O_{4/1}(X1)_{1/1}(X2)_{3/3}]^{7-}\}$ can be observed in the crystal structure of the $Ln_3X_2[As_2O_5][AsO_3]$ representatives, whereas the polyhedra around $(Ln3)^{3+}$ are linked two-dimensionally in the $Ln_5Cl_3[AsO_3]_4$ cases, establishing infinite layers with the composition $^2_\infty\{[Ln3)O_{4/1}(X1)_{1/2}(X2)_{3/3}]^{6.5-}\}$. So despite the structural similarities in both structures, remarkable differences in the coordination spheres of the occurring halide anions lead to different linking patterns of the coordination polyhedra around the involved Ln^{3+} cations.

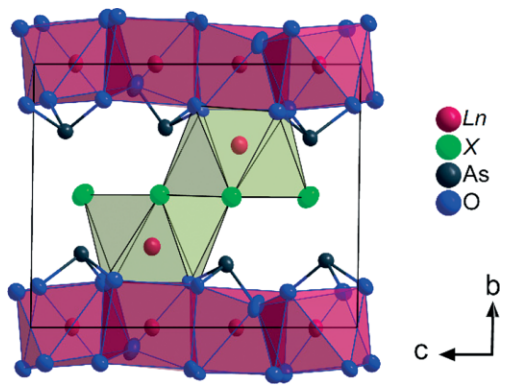

Figure 6. Section of the crystal structure of the $Ln_3X_2[As_2O_5][AsO_3]$ compounds as viewed along [100] with highlighted edges of the unit cell and the refined anisotropic displacement ellipsoids (with an ellipsoid probability of 95 %), emphasizing the edge-connected $[(Ln1,2)O_8]^{13-}$ polyhedra (purple) and the square $[(Ln3)O_4X_4]^{9-}$ antiprisms (greenish for better differentiation).

Crystals of the thulium compound were further examined with electron-beam microprobe methods (see Experimental Section). To investigate the crystal growth and the possible incorporation of silica from the ampoule material or components of the fluxing agent, wavelength dispersive analyses of the crystal surface were performed. A homogeneous distribution of the elements of interest is given, which indicates a uniform crystal growth. During the surface measurements, no significant contents of silicon or cesium were detected as can also be seen from the representative energy dispersive spectrum in Figure 7. Therefore, it can be concluded that no foreign ions deriving from the ampoule material or the fluxing agent are incorporated in the resulting product. The quantification of the WDXS analysis is summarized in Table 4 and confirms the expected composition $Tm_3Br_2As_3O_8$ (≡ $Tm_3Br_2[As_2O_5][AsO_3]$ deriving from the single-crystal refinement).

Powder X-ray diffraction of the $Tm_3Br_2[As_2O_5][AsO_3]$ sample revealed a multiphase composition of the target product. In Figure 8, the collected powder diffractogram is shown with a negative plot of the theoretical pattern deriving from the single-crystal refinement. As main product, the title compound

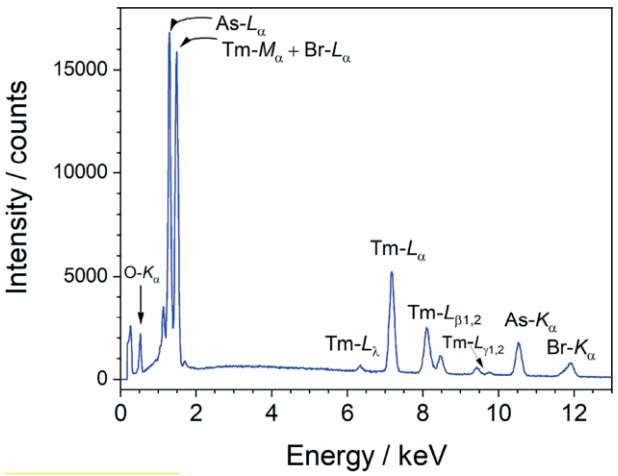

Figure 7. Energy-dispersive X-ray spectrum of $Tm_3Br_2[As_2O_5][AsO_3]$ with designation of the relevant emission lines of the present ions (Tm^{3+}, As^{3+}, Br^- and O^{2-}).

could be identified; however some reflections caused from by-products (marked with stars) are also present. The best accordance of these additional reflections could be achieved with the theoretical pattern of $Tm[AsO_4]$ in the *xenotime*-type structure.[1] Since also a big single crystal of pure arsenic with several millimeters in size could be identified by microprobe measurements, a partial disproportionation of the employed As^{3+} cations to As^{5+} and As^0 seems to have taken place.

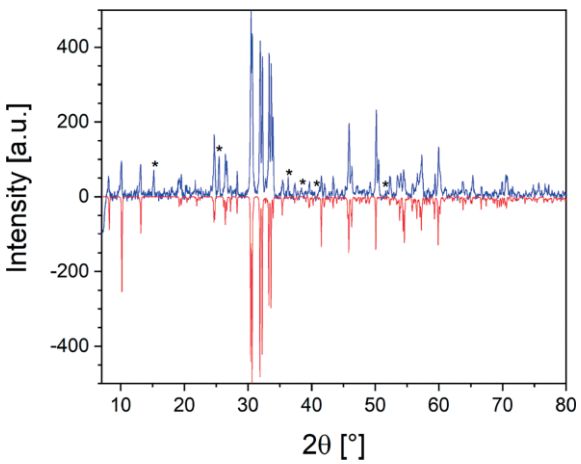

Figure 8. Powder X-ray diffractogram of the gained and water-washed reaction product from a mixture of Tm_2O_3, $TmBr_3$, As_2O_3 and CsBr as starting materials (blue) and the theoretical pattern of $Tm_3Br_2[As_2O_5][AsO_3]$ deriving from the single-crystal refinement (red).

Conclusions

In context to literature-known oxidoarsenates(III) of the lanthanoids, the presented compounds exhibit related structural features. With respect to the occurring coordination numbers of the lanthanoid and arsenic trications, very similar building blocks are found in the presented structures of the new compounds $Ln_3X_2[As_2O_5][AsO_3]$, displaying both isolated and ver-

tex-connected ψ^1-tetrahedra $[AsO_3]^{3-}$ in the form of discrete $[AsO_3]^{3-}$ and pyroanionic $[As_2O_5]^{4-}$ units. As reported in 2005, the quaternary compounds $Ln_5Cl_3[AsO_3]_4$ were the first described halide-containing ones with exclusively isolated ψ^1-tetrahedral $[AsO_3]^{3-}$ anions.[15] In the same year, the first ternary lanthanoid(III) oxidoarsenates(III) $Ln_2As_4O_9$ could be obtained containing both $[As_2O_5]^{4-}$ and $[As_4O_8]^{4-}$ anions[10] as different corner-shared condensation products of $[AsO_3]^{3-}$ pyramids. Compared to the crystal structure of the $Ln_2As_4O_9$ representatives, the pyroanionic $[As_2O_5]^{4-}$ units show a similar conformation in both cases with respect to the non-bonding electron pairs at the arsenic cations, since both electron pairs are pointing into the same direction and not reversed.

Regarding the bridging oxygen atoms in the pyroanionic $[As_2O_5]^{4-}$ units, longer bond lengths compared to the remaining oxygen atoms with contact to only one arsenic cation is observed, which is not unexpected, since an increase of contact numbers should lead to an extension of the bond lengths. However, the present arsenic-oxygen distances are not equally distributed, since in both compounds, $Sm_3Cl_2[As_2O_5][AsO_3]$ and $Tm_3Br_2[As_2O_5][AsO_3]$, the difference between the As1–O3 and the As2–O3 bond lengths accounts to about 10 pm (Table 3), which leads to a remarkably asymmetric $[O_2(As1)–(O3)–(As2)O_2]^{4-}$ anion.

Compared to literature-known ternary or quaternary lanthanoid(III) oxidoarsenates(III), similar structural features, such as the establishment of two-dimensional layers of edge-conntected $[(Ln1,2)O_8]^{13-}$ polyhedra in the crystal structure of the monoclinic $Ln_5Cl_3[AsO_3]_4$[13] representatives or the same conformation of the $[As_2O_5]^{4-}$ pyroanions as in the structure of the $Ln_2As_4O_9$ compounds[10] can be observed. These facts put the presented crystal structures of the compounds $Ln_3X_2[As_2O_5][AsO_3]$ into a coherent general view of the series of already well-understood oxidoarsenates(III) of the rare-earth metals.

Experimental Section

For the synthesis of $Tm_3Br_2[As_2O_5][AsO_3]$, a mixture of the corresponding sesquioxides (Tm_2O_3, ChemPur: 99.999 %; As_2O_3, Grüssing: 99.5 %), thulium tribromide ($TmBr_3$, Aldrich: 99.99 %), and an excess of caesium bromide (CsBr, ChemPur: 99.9 %) were filled into silica ampoules in an argon glove box. The ampoules then were sealed under dynamic vacuum and underwent a defined programme in a high temperature furnace. Over 6 h, the temperature was raised to 780 °C, dwelled for 4 d, cooled to 660 °C over 3 d, dwelled for further 4 d, cooled to 550 °C over 3 d, and then finally quenched to room temperature. The respective chloride-containing samarium compound $Sm_3Cl_2[As_2O_5][AsO_3]$ was synthesized through the solid-state reaction of the particular sesquioxides (Sm_2O_3, ChemPur: 99.9 %; As_2O_3, Sigma: 99.0 %) with an excess of zinc dichloride ($ZnCl_2$, Roth: 98 %) in evacuated silica ampoules. The mixtures were heated to 300 °C within 11 h, dwelled for one day, further heated to 800 °C, dwelled for 30 h, slowly cooled to 400 °C over 70 h and then quenched to room temperature.

After rinsing the reaction mixtures with water in order to remove the fluxing agents, pale yellow, water- and air-stable single crystals of the desired compounds could be selected for both compounds, enabling further characterization with single-crystal diffraction and electron-beam microprobe methods. For X-ray diffraction, selected crystals were put into glass capillaries and fixed with grease on the inner wall. The measurements were performed on a four-circle diffractometer (κ-CCD, Bruker-Nonius) or on a single-circle diffractometer (IPDS-I, Stoe) with monochromatized Mo-K_α radiation at both devices.

The thulium compound was further identified and characterized using electron-beam microprobe techniques. Crystals of adequate size and habit were placed on a conducting carbon pad (Plano G3357) and further underwent a carbon vaporization procedure to avoid surface charging. All experiments were performed on a Cameca SX-100 electron microprobe equipped with five wavelength-dispersive and one energy-dispersive spectrometer. For the quantitative analysis of $Tm_3Br_2As_3O_8$ ($\equiv Tm_3Br_2[As_2O_5][AsO_3]$), the intensity of the characteristic X-ray radiation was measured and quantified using verified standard materials. The emission lines Tm-L_α, As-L_α and Br-K_α were chosen for the quantification, while oxygen was calculated stoichiometrically from the content of the present Tm^{3+}, As^{3+} and Br^- ions. As standard materials for the calibration, $Tm[PO_4]$, GaAs and KBr

Table 1. Crystallographic data of the compounds $Ln_3X_2[As_2O_5][AsO_3]$ with Ln = Sm for X = Cl and Ln = Tm for X = Br.

	$Sm_3Cl_2[As_2O_5][AsO_3]$	$Tm_3Br_2[As_2O_5][AsO_3]$
Crystal system	triclinic	
Space group	$P\bar{1}$ (no. 2)	
Lattice constants:		
a /pm	543.51(4)	534.96(4)
b /pm	837.24(6)	869.27(6)
c /pm	1113.45(8)	1080.79(8)
α /deg	90.084(2)	90.701(2)
β /deg	94.532(2)	94.789(2)
γ /deg	90.487(2)	90.158(2)
Formula units, Z	2	
Calculated density, D_x /g·cm^{-3}	5.752	6.760
Molar volume, V_m /cm^3·mol^{-1}	167.52	150.80
Diffractometer	IPDS-I (STOE, single-circle, image plate detector)	κ-CCD (Bruker-Nonius, four-circle, charge-coupled device-detector)
Wavelength	Mo-K_α (λ = 71.07 pm)	
$F(000)$	766	880
θ_{max} /deg	26.24	27.45
hkl range ($\pm h_{max}$, $\pm k_{max}$, $\pm l_{max}$)	6, 10, 13	6, 11, 13
Observed reflections	6342	21572
Unique reflections	1883	2285
Absorption coefficient, μ /mm^{-1}	27.51	44.18
Absorption correction	numerical, X-SHAPE-99 [33]	
R_{int} / R_σ	0.049 / 0.054	0.066 / 0.026
R_1 / R_1 with $\lvert F_O\rvert \geq 4\sigma(F_O)$	0.040 / 0.027	0.021 / 0.019
wR_2 / GooF	0.054 / 0.877	0.043 / 1.108
Structure determination and refinement	Program package SHELX-97 [34]	
Extinction coefficient, g /10^{-6}·pm^{-3}	–	0.0045(1)
Residual electron density, ρ /e$^-$·10^{-6}·pm^{-3}	1.87 / –1.52	1.08 / –1.15

Table 2. Fractional atomic coordinates and coefficients of the equivalent isotropic displacement parameters of the compounds $Ln_3X_2[As_2O_5][AsO_3]$ with *Ln* = Sm for *X* = Cl (top) and *Ln* = Tm for *X* = Br (bottom; all atoms occupy the general *Wyckoff* site 2*i*).

Atom	x / a	*y* / *b*	*z* / *c*	U_{eq} /pm^2
Sm1	0.24303(9)	0.00568(6)	0.36972(4)	104(1)
Sm2	0.26600(9)	0.99703(6)	0.87216(4)	105(1)
Sm3	0.26824(9)	0.33785(6)	0.63167(4)	133(1)
Cl1	0.3048(5)	0.5150(3)	0.83972(19)	182(6)
Cl2	0.2300(5)	0.4924(3)	0.38908(19)	145(5)
As1	0.18672(19)	0.71213(12)	0.15609(7)	116(2)
As2	0.18164(19)	0.27102(12)	0.08883(7)	106(2)
As3	0.27777(19)	0.74561(12)	0.58911(7)	109(2)
O1	0.4387(13)	0.8256(8)	0.2217(5)	139(15)
O2	0.0245(13)	0.1894(8)	0.7474(5)	102(15)
O3	0.0622(13)	0.8349(7)	0.0258(5)	91(14)
O4	0.4166(13)	0.1480(8)	0.0403(5)	153(16)
O5	0.0915(13)	0.1476(8)	0.2049(5)	132(15)
O6	0.3603(13)	0.9062(8)	0.6844(5)	171(16)
O7	0.0155(13)	0.8308(8)	0.5081(5)	122(15)
O8	0.4980(13)	0.8169(7)	0.4849(5)	101(14)
Atom	x / a	*y* / *b*	*z* / *c*	U_{eq} /pm^2
Tm1	0.24704(4)	0.00003(3)	0.37102(2)	93.3(8)
Tm2	0.26454(4)	0.00269(3)	0.87266(2)	92.0(8)
Tm3	0.26456(4)	0.30786(3)	0.63165(2)	107.6(8)
Br1	0.30172(11)	0.50478(6)	0.84510(5)	162.9(13)
Br2	0.23078(11)	0.49554(6)	0.38983(5)	147.3(13)
As1	0.19064(11)	0.72049(6)	0.15175(5)	89.7(12)
As2	0.18288(11)	0.25530(6)	0.09807(5)	93.9(12)
As3	0.27809(11)	0.75946(6)	0.59570(5)	94.4(12)
O1	0.4485(7)	0.8276(4)	0.2221(3)	114(8)
O2	0.0185(7)	0.1801(4)	0.7469(3)	96(7)
O3	0.0630(7)	0.8439(4)	0.0220(3)	112(8)
O4	0.4143(7)	0.1355(4)	0.0445(3)	108(8)
O5	0.0795(7)	0.1355(4)	0.2134(3)	105(8)
O6	0.3736(7)	0.9187(4)	0.6895(3)	140(8)
O7	0.0108(7)	0.8427(4)	0.5087(3)	89(7)
O8	0.4987(7)	0.8288(4)	0.4857(3)	94(7)

Table 3. Selected interatomic distances (*d* /pm, *e.s.d.*: ±0.3) for the compounds $Ln_3X_2[As_2O_5][AsO_3]$ with *Ln* = Sm for *X* = Cl (left) and *Ln* = Tm for *X* = Br (right).

	$Sm_3Cl_2[As_2O_5][AsO_3]$	$Tm_3Br_2[As_2O_5][AsO_3]$
*Ln*1–O1	253.3	250.0
*Ln*1–O2	247.7	239.4
*Ln*1–O5	228.9	221.1
*Ln*1–O6	239.5	230.0
*Ln*1–O7	245.6	239.3
*Ln*1–O7′	251.5	245.7
*Ln*1–O8	241.4	231.1
*Ln*1–O8′	253.1	245.9
*Ln*2–O1	247.0	242.2
*Ln*2–O2	245.0	239.2
*Ln*2–O3	250.5	245.2
*Ln*2–O3′	261.1	254.1
*Ln*2–O4	227.5	223.1
*Ln*2–O4’	234.6	226.2
*Ln*2–O5	238.2	231.8
*Ln*2–O6	232.0	222.5
Ln3–O1	259.0	242.7
*Ln*3–O2	228.2	219.5
*Ln*3–O7	252.4	239.9
*Ln*3–O8	229.4	220.5
Ln3–*X*1	274.2	284.9
Ln3–*X*2	299.0	309.1
Ln3–*X*2′	306.2	315.1
Ln3–*X*2″	308.9	321.7
As1–O1	176.9	177.5
As1–O2	183.3	184.0
As1–O3	186.6	186.1
As2–O3	197.0	195.9
As2–O4	175.3	175.1
As2–O5	176.5	175.8
As3–O6	174.5	175.5
As2–O7	178.1	180.3
As2–O8	182.9	184.9

found application. The raw counting values were corrected using Pouchou and Pichoir's matrix correction algorithm "PaP"[35,36] to receive the mass- and atomic contents of the involved ions.

Powder X-ray diffraction was performed on a STOE Stadi-P diffractometer with Cu-K_α radiation, transmission geometry and a STOE image-plate detector. As monochromator, a curved germanium crystal with diffraction active (111) face was used. To minimize texture effects, the sample was crushed to obtain a homogeneous powder and measured under permanent rotation. Data collection was performed with 20 min of exposure time. Crystallographic data and structure refinement results are summarized in Table 1 and atom positions are listed in Table 2. Selected interatomic distances are summarized in Table 3. Electron-beam microprobe phase analysis data are given in Table 4.

Crystallographic data (including structure factors) for the structures in this paper have been deposited with the Cambridge Crystallographic Data Centre, CCDC, 12 Union Road, Cambridge CB21EZ, UK. Copies of the data can be obtained free of charge on quoting the depository numbers CCDC-1944725 for $Sm_3Cl_2[As_2O_5][AsO_3]$ and CCDC-1902725 for $Tm_3Br_2[As_2O_5][AsO_3]$ (Fax: +44-1223-336-033; E-Mail: deposit@ccdc.cam.ac.uk, http://www.ccdc.cam.ac.uk)

Table 4. Electron-beam microprobe phase analysis of $Tm_3Br_2[As_2O_5][AsO_3]$ crystals using 20 kV acceleration voltage and wavelength dispersive spectrometry.

Element	Oxidation state	Experimental content /wt-%	Experimental content /atom-%	Theoretical content /atom-%
Tm	+3	21.80(7)	18.5(1)	18.75
Br	–1	15.4(1)	12.57(9)	12.50
As	+3	47.9(3)	18.97(6)	18.75
O	–2	12.3(2)	49.9(3)	50.00

Acknowledgements

We thank *Dr. Falk Lissner* (Stuttgart) and *Dipl.-Chem. Wolfgang Saak* (Oldenburg) for the single-crystal X-ray diffraction measurements.

Keywords: Lanthanoids; Rare-earth metal compounds; Halide oxidoarsenates(III); Structure elucidation; Solid-state synthesis

References

[1] H. Schwarz, *Z. Anorg. Allg. Chem.* **1963**, *323*, 44–56.
[2] P. Emsbo, P. I. McLaughlin, G. N. Breit, E. A. Du Bray, A. E. Koenig, *Gondwana Res.* **2015**, *27*, 776–785.
[3] Y. Ni, J. M. Hughes, A. N. Mariano, *Am. Mineral.* **1995**, *80*, 21–26.
[4] F. X. Zhang, M. Lang, R. C. Ewing, J. Lian, Z. W. Wang, J. Hu, L. A. Boatner, *J. Solid State Chem.* **2008**, *181*, 2633–2638.
[5] A. Tymiński, T. Grzyb, *J. Lumin.* **2017**, *181*, 411–420.
[6] M. Strada, G. Schwendimann, *Gazz. Chim. Ital.* **1934**, *64*, 662–674.
[7] S. J. Metzger, F. Ledderboge, G. Heymann, H. Huppertz, Th. Schleid, *Z. Naturforsch. B* **2016**, *71*, 439–445.
[8] F. Ledderboge, J. Nowak, H.-J. Massonne, K. Förg, H. A. Höppe, Th. Schleid, *J. Solid State Chem.* **2018**, *263*, 65–71.
[9] M. Ben Hamida, C. Warns, M. S. Wickleder, *Z. Naturforsch. B* **2005**, *60*, 1219–1223.
[10] D.-H. Kang, Th. Schleid, *Z. Anorg. Allg. Chem.* **2006**, *632*, 91–96.
[11] S. J. Metzger, G. Heymann, H. Huppertz, Th. Schleid, *Z. Anorg. Allg. Chem.* **2012**, *638*, 1119–1122.
[12] F. Ledderboge, S. J. Metzger, G. Heymann, H. Huppertz, Th. Schleid, *Solid State Sci.* **2014**, *37*, 164–169.
[13] F. C. Goerigk, M. Ben Hamida, D.-H. Kang, F. Ledderboge, S. Schander, Th. Schleid, M. S. Wickleder, *Z. Naturforsch. B* **2019**, *74*, 497–506.
[14] D.-H. Kang, Th. Schleid, *Z. Kristallogr.* **2007**, *S 25*, 98.
[15] M. Ben Hamida, M. S. Wickleder, *Z. Anorg. Allg. Chem.* **2006**, *632*, 2195–2197.
[16] F. Ledderboge, Oxo- und Thioarsenate(III/V) der Seltenerdmetalle, Doctoral Dissertation, Universität Stuttgart, Germany **2016**.
[17] H. Ben Yahia, U. C. Rodewald, R. Pöttgen, *Z. Naturforsch. B* **2009**, *64*, 896–900.
[18] D.-H. Kang, Th. Schleid, *Z. Anorg. Allg. Chem.* **2007**, *633*, 1205–1210.
[19] H. Ben Yahia, R. Pöttgen, U. C. Rodewald, *Z. Naturforsch. B* **2010**, *65*, 1289–1292.
[20] D.-H. Kang, Oxoarsenate(III/V) und Thioarsenate(III) der Selten-Erd-Metalle, Dissertation, Stuttgart, Germany **2009**.
[21] H. Ben Yahia, A. Villesuzanne, U. C. Rodewald, Th. Schleid, R. Pöttgen, *Z. Naturforsch. B* **2010**, *65*, 549–555.
[22] D.-H. Kang, J. Wontcheu, Th. Schleid, *Solid State Sci.* **2009**, *11*, 299–304.
[23] D. H. Templeton, C. H. Dauben, *J. Am. Chem. Soc.* **1953**, *75*, 6069–6070.
[24] A. Bartos, K. P. Lieb, M. Uhrmacher, D. Wiarda, *Acta Crystallogr., Sect. B* **1993**, *49*, 165–169.
[25] H. Ishibashi, K. Shimomoto, K. Nakahigashi, *J. Phys. Chem. Solids* **1994**, *55*, 809–814.
[26] I. Mayer, S. Zolotov, F. Kassierer, *Inorg. Chem.* **1965**, *4*, 1637–1639.
[27] G. Meyer, Th. Schleid, *J. Less-Common Met.* **1986**, *116*, 187–197.
[28] D. Brown, S. Fletcher, D. G. Holah, *J. Chem. Soc. A* **1968**, 1889–1894.
[29] M. Priestner, G. Singer, M. Weil, R. K. Kremer, E. Libowitzky, *J. Solid State Chem.* **2019**, *277*, 209–215.
[30] F. Pertlik, *Monatsh. Chem.* **1978**, *109*, 277–282.
[31] F. Pertlik, *Monatsh. Chem.* **1975**, *106*, 755–762.
[32] P. Ballirano, A. Maras, *Z. Kristallogr. – New Cryst. Struct.* **2002**, *217*, 177–178.
[33] STOE & Cie GmbH Darmstadt, STOE X-SHAPE Crystal Optimization for Numerical Absorption Correction **1999**.
[34] G. M. Sheldrick, SHELX-97 Program Package for Single-Crystal Structure Solution and Refinement of X-ray Diffraction Data, Göttingen **1997**.
[35] J.-L. Pouchou, F. Pichoir, in: *Electron Probe Quantitation* (Eds.: K. F. J. Heinrich, D. E. Newbury), Plenum Press, New York **1991**, 31–75.
[36] J.-L. Pouchou, F. Pichoir, *Rech. Aerosp.* **1984**, *3*, 167–192.

Received: December 27, 2019